Facilitated transport of a PAH mixture by a rhamnolipid biosurfactant in porous silica matrices

Noordman, WH; Bruining, JW; Wietzes, P; Janssen, DB; Bruining, Jaap-Willem

Published in:
Journal of Contaminant Hydrology

DOI:
10.1016/S0169-7722(00)00097-8

Publication date:
2000

ELSEVIER

Journal of Contaminant Hydrology 44 (2000) 119–140

JOURNAL OF Contaminant Hydrology

www.elsevier.com/locate/jconhyd

Facilitated transport of a PAH mixture by a rhamnolipid biosurfactant in porous silica matrices

Wouter H. Noordman [1], Jaap-Willem Bruining [2], Pieter Wietzes, Dick B. Janssen *

Department of Biochemistry, Groningen Biomolecular Sciences and Biotechnology Institute, University of Groningen, Nijenborgh 4, 9747 AG Groningen, Netherlands

Received 26 August 1999; received in revised form 7 April 2000; accepted 10 April 2000

Abstract

The facilitated transport of a mixture of three polycyclic aromatic hydrocarbons (PAH) (naphthalene, fluorene, and phenanthrene) by a rhamnolipid biosurfactant was determined with silica, octadecyl-coated silica, and humic acid-coated silica columns. The retardation factors for the contaminants in the absence of rhamnolipid ranged from 1.8 (naphthalene with silica) to 708 (phenanthrene with octadecyl-coated silica). The retardation factors for phenanthrene were up to eightfold lower in the presence of 500 mg/l rhamnolipid compared to the situation where no rhamnolipid was present. The facilitated transport of the contaminants in the presence of rhamnolipid could be predicted by accounting for sorption, solubilization and admicellar sorption. In the octadecyl-coated matrix, transport of fluorene and phenanthrene was enhanced even in the presence of sub-micellar solution of rhamnolipid (20 mg/l), showing that adsorbed surfactant reduced the affinity of these compounds to this stationary phase. Linear free-energy relations (LFERs) indicated that the matrix–water, micelle–water, and admicelle–water partitioning constants for PAH were correlated with their 1-octanol–water partitioning constants. These correlations were used to simulate the facilitated transport of contaminants of varying hydrophobicity by a surfactant. It was concluded that surfactants have the greatest transport facilitating effect on the more hydrophobic components. The effectiveness of surfactants for enhancing removal of the less hydrophobic compounds ($\log K_{ow} < 3.4$) may considerably be reduced due to admicellar sorption.

Keywords: Surfactant; Biosurfactant; Contaminant transport; Porous media; Adsorption

* Corresponding author. Tel.: +31-50-363-4209; fax: +31-50-363-4165.
E-mail address: d.b.janssen@chem.rug.nl (D.B. Janssen).
[1] Currently at: Hercules European Research Center, Barneveld, The Netherlands.
[2] Currently at: Shell, Pernis, The Netherlands.

0169-7722/00/$ - see front matter
PII: S0169-7722(00)00097-8

1. Introduction

The prospects for the use of (bio)surfactants in soil remediation are dependent on the capacity of these compounds to enhance desorption or dissolution of contaminants, to increase the rate of transport of contaminants in soil, and to stimulate biodegradation. These factors may be related, since enhanced desorption, dissolution, or transport may increase the bioavailability of the contaminant and hence increase biodegradation rates. Surfactants have been applied for stimulating the dissolution of non-aqueous phase liquids initially present in soil (Bai et al., 1997; Fortin et al., 1997), the dissolution of solid contaminants (Mulder et al., 1998), and the desorption and transport of soil-sorbed contaminants (Edwards et al., 1994; Noordman et al., 1998). This paper focuses on biosurfactant-enhanced transport of sorbed contaminants. Surfactants may facilitate the transport of hydrophobic contaminants by solubilizing these compounds (Edwards et al., 1994; Noordman et al., 1998). However, surfactants may also retard the transport of contaminants due to the partitioning of contaminants to an adsorbed surfactant phase (Park and Jaffé, 1993; Monticone et al., 1994; Sun et al., 1995). Furthermore, surfactants can increase desorption rate constants of contaminants, presumably by inducing swelling of the soil organic matter (Sahoo and Smith, 1997; Noordman et al., 1998). To allow a prediction of the surfactant-enhanced transport of adsorbed contaminants, a more detailed insight is needed into the importance of the interactions between (adsorbed) surfactant, contaminant, and soil.

The objective of this research was to obtain insight in the effect of surfactants on the sorption, solubilization and admicellar sorption of hydrophobic contaminants. Therefore, three types of model matrices were used. A silica matrix was used to represent mineral surfaces in soil and as a reference matrix for the other two. The hydrophobic octadecyl derivatized silica (ODS) was used since sorption to this matrix is determined by hydrophobic interactions, as is also the case for most soils. The retention of a compound on an ODS column can be used to determine its soil–water distribution constant (Chin et al., 1988; Szabó and Bulman, 1994), which emphasizes its suitability as a model matrix. Humic acid derivatized silica (HAS) was used because retardation of hydrophobic contaminants in real soils is determined to a great extent by humic material. HAS was found to be a valuable model matrix for determining soil–water partitioning constants (Szabó and Bulman, 1994; Nielsen et al., 1997). Silica, ODS, and HAS have been used previously for the study of sorption processes of soil contaminants (Szecsody and Bales, 1989; Burris et al., 1991; Huang and Weber, 1997b). These matrices allowed determination of the sorption processes in well-defined, homogeneous situations in the absence of non-equilibrium effects.

The rhamnolipid biosurfactant produced by several *Pseudomonas* strains was chosen for our studies because this surfactant was effective at enhancing removal of sorbed phenanthrene from soil columns (Noordman et al., 1998). Interactions between this surfactant, a mixture of three polycyclic aromatic hydrocarbons (PAH), and the model matrices were investigated using column studies by measuring retardation factors for the PAHs as a function of the concentration of rhamnolipid in the background solution. Batch experiments were used to determine micelle–water partitioning constants. Matrix–water partitioning constants for PAH were derived from column experiments

without surfactant present and were compared to constants that were determined in batch experiments. LFERs were used to relate sorption, admicellar sorption, and solubilization of the PAHs to the 1-octanol–water partitioning constant of these contaminants. By combining these relationships, a description of the interactions between surfactant, contaminants, and a matrix was obtained that was used to make a general prediction of surfactant-enhanced transport.

2. Materials and methods

2.1. Chemicals and solutions

Naphthalene, fluorene, phenanthrene ($\geq$ 99% purity), and pentafluorobenzoic acid (99%) were obtained from Acros (Geel, Belgium). In all experiments, a background electrolyte solution was used, which contained 3 mM NaN_3 to suppress microbial activity and 10 mM Tris–HCl, pH 7.0, in triple distilled water. PAH-containing solutions were prepared by injection of 0.5 ml of a methanolic stock solution into 1-l water yielding a solution containing 7 mg/l naphthalene, 1 mg/l fluorene, and 1 mg/l phenanthrene.

2.2. Matrices

Silica (pore size 60 Å, particle size 43–60 μm) was obtained from Merck and used after extensive washing with 0.1 M HCl, methanol, and water to remove potential impurities, and after drying overnight at 150°C (Szecsody and Bales, 1989). ODS was obtained from Baker (Bakerbond C18 polar plus, pore size 60 Å, particle size 40 μm). HAS was prepared by covalently coating humic acid (Acros) to silica by diazotation using a five-step procedure (Szabó et al., 1993). The humic acid content of the humic acid-coated silica (HAS) was determined to be 2.2% C, 1.1% H, 0.4% N, and 5.1% O using elemental analysis and as 4.2% humic acid (w/w) using an alkaline hydrolysis assay with Acros humic acid as a standard (Klavins, 1993). These values are equivalent, given that the carbon content of humic acid is approximately 50% (w/w) (Klavins, 1993; Schwarzenbach et al., 1993; Huang and Weber, 1997a). Products of the intermediate synthesis steps did not give significant response with the alkaline hydrolysis assay. Less than 1% of the humic acid was removed from HAS during incubation in electrolyte solution for 8 days, as was determined by colorimetric analysis of the supernatant, indicating that negligible amounts of humic acid leached from HAS during the column experiments.

2.3. Rhamnolipid

Rhamnolipid was produced by *Pseudomonas aeruginosa* UG2, isolated from the culture fluid by a series of consecutive steps of acid precipitation and dissolution in 50 mM $NaHCO_3$, and purified by column chromatography over Sephadex LH20 with methanol as the eluent (Noordman et al., 2000). HPLC analysis showed that this biosurfactant mixture contained six rhamnolipid components (Noordman et al., 2000).

2.4. Column studies

An all-glass column with adjustable glass shaft (0–20 cm length, 2.5 cm i.d.), a glass inlet frit (Schott, type P4), and a stainless steel outlet frit (0.5 μm pore diameter, Alltech Associated) was custom built to ensure low sorption of the compounds to the apparatus (Lion et al., 1990). Columns containing silica or HAS were dry packed in a single step and consolidated by using vibration. Columns containing ODS were packed by filling 4.9-g silica and 80-mg ODS into a column with an enlarged bed volume, and fluidizing the bed with nitrogen gas for 2 h. After this mixing step, the bed volume was minimized. After packing, the columns were wetted with electrolyte solution until saturation was complete. This was determined gravimetrically and by visual inspection. The bulk density ρ and porosity θ were determined gravimetrically and were found to be 0.5 kg matrix/l column volume and 0.7–0.8 l aq phase/l column volume, respectively. A manually operated six-port stainless steel valve was placed in line of the column influent to facilitate switching between different solutions. The air entering the influent reservoir to replace the PAH-containing electrolyte solution that was delivered to the column was saturated with PAH by leading it through an aqueous solution with an equimolar PAH concentration. A peristaltic pump with Marprene II tubing (tube bore 1.6 mm, wall 0.8 mm, Watson–Marlow, Falmouth Cornwall UK) was used to control the flow and was either placed downstream or upstream of the column. In the latter case, separate tubing was used for PAH-containing and PAH-free solutions and the tubing was equilibrated with the solution before the start of the experiment. Flow rates were determined volumetrically and were 0.25 ml/min for all experiments, resulting in a pore water velocity of 4 cm/h. Stainless steel tubing (0.8 mm i.d.) was used for all connections. The column was thermostated using a water jacket connected to a water bath. The temperature inside the water jacket was determined to be 25.0 ± 0.5°C using an electronic sensor.

The column effluent was passed through a six-way rheodyne HPLC valve equipped with a 175-μl injection loop and connected to an HPLC system. The valve was operated by an actuator (Thar, Alltech), which was controlled by the HPLC pump. This set-up allowed on-line HPLC analysis of PAH (dissolved plus micelle-partitioned) and of rhamnolipid, both with an experimental error of maximally 3%. Analysis of PAH and rhamnolipid did not interfere and all PAHs and rhamnolipid components could be analyzed simultaneously. The HPLC set-up consisted of a Merck L-6200 HPLC pump (Hitachi), a Chromsphere PAH 100 mm column (Chrompack), a Merck L-4200 UV–VIS detector (Hitachi) for detection of PAH at 254 nm, and an evaporative light scattering detector (MARK III, Varex, Burtonsville, USA) for detection of rhamnolipid. The mobile phase used for analysis of PAH consisted of 55% acetonitrile (v/v) and 45% water (v/v). For analysis of rhamnolipid, 0.03% trifluoroacetic acid (v/v) was added to this mobile phase. This addition did not affect the chromatograms of the PAHs. The flow rate was 0.5 ml/min. Data were collected with a Kontron LC data analysis package (version 3.90, Kontron Instruments, Milan, Italy) running on a PC. Breakthrough curves for the conservative tracer pentafluorobenzoic acid were analyzed using the Merck L-4200 UV–VIS detector at 250 nm placed in line of the column effluent. The total recovery of PAH varied from 97% to 104%.

2.5. Matrix–water partitioning constants

The equilibrium distribution constants (K_d) for sorption of phenanthrene to ODS and HAS were determined by adding samples of 12–25 mg of a mixture of ODS and silica (1.6% octadecyl-coated silica in silica (w/w), the same mixture as used for the column experiments) or 20–100 mg of HAS to a 5-ml solution containing 1 mg/l phenanthrene (C_{init}, mg/l) in 8-ml pyrex tubes that were closed with aluminum-coated septa. After incubation for 48 h (ODS) or 170 h (HAS) by end-over-end rotation (18 rpm, room temperature), the incubation vessels were centrifuged at 4000 rpm for 5 min and the supernatant was analyzed for phenanthrene (C_{final}, mg/l) by UV absorbance at 250 nm. A distribution ratio D was calculated at each solid concentration (S_c, kg ODS or kg HAS/l solution) as $D = (C_{init} - C_{final})/(S_c C_{final})$. The equilibrium distribution constants (K_d) were calculated as the average of the distribution ratios.

2.6. Solubilization

Solutions containing 0–700 mg/l rhamnolipid were saturated with naphthalene, fluorene, or phenanthrene by repeated application to a column packed with Chromosorb GAW (Chrompack, Bergen op Zoom, The Netherlands) that was coated with the respective PAH (Noordman et al., 1998). The critical micelle concentration (CMC, g/l) and the three micelle–water partitioning constants (K_c, mass-based micelle–water partitioning constant (l/g, Noordman et al., 1998) were determined by fitting the combined solubility data for naphthalene, fluorene and phenanthrene to Eq. (1) using the program Scientist (version 2.0 for Windows, Micromath Scientific, Salt Lake City, UT).

$$C = {}_{PAH,t} = C_{PAH,aq}(1 + K_c C_{mic})$$
$$C_{mic} = C_{surf} - \mathrm{CMC} \text{ when } C_{surf} > \mathrm{CMC}$$
$$C_{mic} = 0 \text{ when } C_{surf} \leq \mathrm{CMC} \quad (1)$$

where $C_{PAH,t}$ is the total concentration of a PAH in the aqueous phase (dissolved plus solubilized, g/l), $C_{PAH,aq}$ the concentration of a dissolved PAH (g/l), and C_{surf} is the aqueous surfactant concentration (g/l).

2.7. Quantitative analysis

Breakthrough curves of the conservative tracer pentafluorobenzoic acid were analyzed with a local equilibrium advective–dispersive transport model to determine the Peclet number using the computer program CXTFIT (Parker and Van Genuchten, 1984). The retardation factors for the individual rhamnolipid components and for the PAHs were determined from the first central moment corrected for a final pulse (Das and Kluitenberg, 1996). The retardation factors for the PAHs in the presence of 20 mg/l rhamnolipid in the experiment with the ODS column were determined by optimization using the computer program CXTFIT with R as the sole fitting parameter, since the experiment was terminated before the components were fully eluted from the column.

The adsorbed concentration of rhamnolipid (S_{surf}, mg rhamnolipid/kg soil) in columns saturated with rhamnolipid was calculated as the total amount of surfactant bound to the matrix from the retardation factors for the individual rhamnolipid components using $S_{surf} = \sum_i \theta/\rho(R_i - 1)m_i C_{RL}$ where R_i is the retardation factor for component i, m_i is the mass fraction of component i in the rhamnolipid mixture as determined by HPLC, and C_{RL} is the aqueous rhamnolipid concentration in the column (g/l).

3. Results and discussion

3.1. Characterization of the columns using a conservative tracer

The hydrodynamic properties of columns packed with silica, ODS, and HAS were determined by using the conservative tracer pentafluorobenzoic acid. Breakthrough curves of pentafluorobenzoic acid were sigmoidal in shape and showed no tailing. Furthermore, Peclet numbers were higher than 100 for columns packed with silica and ODS and higher than 50 for columns packed with HAS. This indicated that physical non-equilibrium effects were absent and that all columns were packed homogeneously. Breakthrough curves of pentafluorobenzoic acid that were determined after prolonged operation of the columns indicated that column integrity remained intact. The retardation factor for pentafluorobenzoic acid in silica was 0.6 when the standard electrolyte solution was used, but 1.0 when a solution with a higher ionic strength was used (standard electrolyte solution supplemented with 20 mM KCl or 100 mM $CaCl_2$). This indicated that pentafluorobenzoic acid was partially excluded from the negatively charged silica pores due to anion exclusion. Since the dispersion constant for pentafluorobenzoic acid was independent of the electrolyte concentration, movement of the tracer through the silica pores was fast compared to the hydrodynamic residence time.

3.2. Transport of PAH

3.2.1. Transport of PAH in the absence of rhamnolipid

Transport of a mixture of PAHs containing naphthalene, fluorene, and phenanthrene through columns packed with silica, ODS, and HAS was determined by measuring breakthrough curves. Experiments performed with an empty column showed that sorption of the PAHs to the column itself and tubing was minimal. Therefore, the observed retardation of PAHs in experiments with columns that were packed with matrices was fully caused by sorption to the matrix. Several experiments with silica columns that were performed in duplicate showed less than 6% variation in retardation factors. The breakthrough curves of PAH were symmetrical with all three porous matrices (Fig. 1). This indicates that sorption isotherms were linear, as was found previously for ODS (Huang and Weber, 1997b) and HAS (Burris et al., 1991).

Retardation factors increased with increasing solute hydrophobicity in the order of naphthalene < fluorene < phenanthrene (Table 1). Retardation factors for the PAHs in ODS and HAS were considerably larger than for silica, indicating that PAH retardation in the ODS and HAS columns was mainly determined by the octadecyl and humic acid coatings, respectively. The retardation factor for phenanthrene in the ODS column was

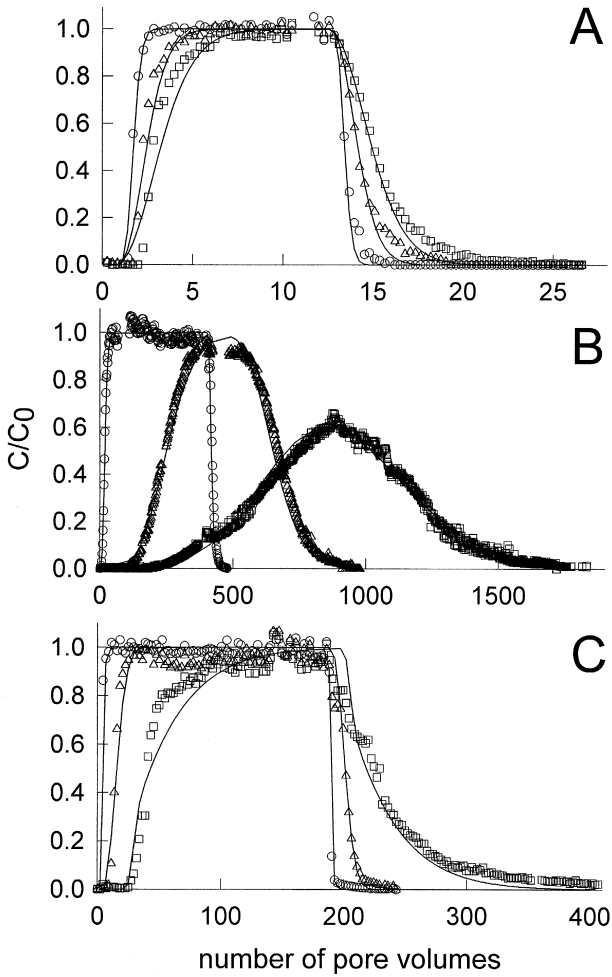

Fig. 1. Transport of PAH in the different model matrices. Breakthrough curves of naphthalene (○), fluorene (△), and phenanthrene (□) for silica (A), ODS (B), and HAS (C). C_0 is the influent concentration of the individual PAHs (g/l). Line indicates the fit of the data to an advective–dispersive transport model with one rate-limited domain (A and B) or one rate-limited and one equilibrium domain (C) using the Damkohler number as the sole fitting parameter.

large and the determination of the value required 1800 pore volumes or 6 weeks of continuous column operation (Fig. 1C), even though a mixture of ODS and silica was used for these experiments. The retardation factors for naphthalene, fluorene, and phenanthrene in ODS were calculated to be 50, 315, and 760 from a relationship published by Khaledi and Breyer (1989) and by accounting for the mass fraction of ODS in the ODS column. Buszewski et al. (1997) predict a retardation factor of 1283 for naphthalene with an ODS column eluted with a purely aqueous mobile phase. This corresponds to a retardation factor of 21.5 in an ODS column with 1.6% ODS (w/w).

Table 1
Effect of rhamnolipid on the retardation factors for the PAHs with different matrices

Matrix	[RL][a] (mg/l aq phase)	[RL][b] (mg/kg matrix)	Retardation factor					
			Naphthalene		Fluorene		Phenanthrene	
			Observed	Predicted[c]	Observed	Predicted[c]	Observed	Predicted[c]
Silica	0	0	1.75		2.58		3.45	
	20	1.0×10^{2}	1.90	1.82	2.61	2.81	3.73	4.13
	50	1.0×10^{2}	1.86	1.78	2.45	2.60	3.68	3.32
	150	1.0×10^{2}	1.62	1.70	2.33	2.20	3.15	2.27
	285	0.9×10^{2}	1.37	1.62	NA[d]	1.90	1.43	1.80
	500	0[e]	1.76	1.48	1.38	1.56	1.19	1.38
ODS[f]	0	0	19.8		258		708	
	20	1.1×10^{3}[g]	44[h]	21.0	119[h]	267	257[h]	732
	500	2.9×10^{3}[g]	20.3	14.4	67.3	94.4	89.5	114
HAS	0	0	4.55		19.1		54.5	
	500	9.1×10^{3}	11.3	7.84	21.4	15.6	22.7	20.0

[a] Concentration of rhamnolipid in the aqueous phase.
[b] Concentration of rhamnolipid adsorbed to the matrix.
[c] Predicted retardation factors were calculated as described in Section 3.4.1.
[d] Not applicable since this experiment was performed with a mixture of naphthalene and phenanthrene.
[e] $R_{surf} < 1$.
[f] Column packed with 1.6 wt.% octadecyl-coated silica in silica.
[g] mg rhamnolipid/kg ODS–silica mixture.
[h] Since the experiment was terminated before the components were fully eluted from the column, retardation factors were determined by optimization using the computer program CXTFIT with R as the sole fitting parameter.

The good agreement between the observed retardation factors for PAH in ODS (Table 2) and the literature data suggests that the large retardation factors, which were found for the PAHs in the ODS columns were realistic.

Matrix–water partitioning constants (K_d) could be determined from the observed retardation factors for PAH (R) using Eq. (2), which is valid for compounds with a linear sorption isotherm.

$$R = 1 + \frac{\rho}{\theta} K_d \tag{2}$$

The resulting matrix–water partitioning constants for phenanthrene with ODS and HAS corresponded well to the values determined in batch equilibration experiments using the ODS–silica mixture ($\log K_d = 3.10$) and HAS ($\log K_d = 1.97$) (Table 2).

Partitioning constants normalized to the organic-carbon content of the matrix (K_{oc}, l/kg organic carbon) were obtained by dividing the matrix–water partitioning constants by the organic carbon content of the matrices (kg organic carbon/kg matrix). These constants were up to two orders of magnitude higher for ODS than for HAS (Table 2). This difference between ODS and HAS reflects the much higher hydrophobicity of the octadecyl coating compared to the humic acid coating, which is thought to be caused by the presence of polar and ionic moieties in HAS. This is similar to the observed decrease in K_{oc} with increase in O/C ratio in soil organic matter (Huang and Weber, 1997a). It

Table 2
Partitioning constants for naphthalene, fluorene, and phenanthrene. Intercepts and slopes are given for the log–log plots of the partitioning constants vs. K_{ow}

	1-octanol	Silica	ODS[a]		HAS		Rhamnolipid	
	log K_{ow}	log K_d	log K_d	log K_{oc}^b	log K_d	log K_{oc}^b	log K_c^c	log K_{oc}^b
Naphthalene	3.36	0.085	1.51	4.03	0.735	2.32	0.06	2.83
Fluorene	4.18	0.408	2.64	5.18	1.36	3.01	0.58	3.35
Phenanthhrene	4.57	0.599	3.09	5.63	1.87	3.55	1.06	3.83
r^{2d}		0.997	0.998		0.992		0.97	
Intercept[d]		−1.33	−2.89		−2.54		−2.64	
Slope[d]		0.42	1.31		0.955		0.794	

[a]Mixture of octadecyl-coated silica and silica containing 1.6% octadecyl-coated silica (w/w).

[b]Organic carbon-normalized partitioning constants (K_{oc}, l/kg) calculated as $K_{oc} = K_d / f_{oc}$ or $K_{oc} = K_c / f_{oc}$ where f_{oc} is the organic carbon content. The values for f_{oc} were 0.0029, 0.02, and 0.59 g/g for the mixture of octadecyl-coated silica and silica (ODS), HAS, and rhamnolipid, respectively.

[c]K_c values were determined as 1.15 ± 0.03, 3.8 ± 0.3, and 11.4 ± 0.3 l/g , for naphthalene, fluorene, and phenanthrene, respectively.

[d]Value for r^2 for the correlation of log K_d, log K_m, and log K_c with log K_{ow}, and the intercept and slope of the corresponding plots.

can be concluded that sorption of PAH to ODS and HAS is dependent on the amount and type of organic carbon present in these matrices.

3.2.2. Facilitated transport of PAH

The effect of rhamnolipid on the transport of PAH was determined by measuring the breakthrough curves of PAH in columns pre-equilibrated with rhamnolipid (20–500 mg/l) and by comparing these to the breakthrough curves of PAH in the absence of rhamnolipid (the control). At rhamnolipid concentrations of 20 and 50 mg/l, transport of PAH in silica was retarded as compared to the control (Table 1, Fig. 2). In contrast,

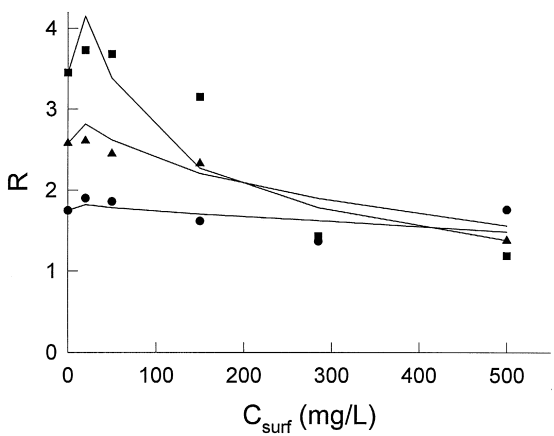

Fig. 2. Effect of rhamnolipid on the retardation factors for naphthalene (●), fluorene (▲), and phenanthrene (■) in silica. The solid line indicates the retardation factors predicted using Eq. (3) as explained in the text.

transport of phenanthrene and fluorene in ODS was remarkably facilitated in the presence of 20 mg/l rhamnolipid (Table 1). In the presence of 500 mg/l rhamnolipid, the mobility of phenanthrene was enhanced compared to the control for all three matrices (Table 1, Fig. 3). In the ODS column, an eight-fold enhancement was observed. Transport of phenanthrene was enhanced to a greater extent than the transport of the less hydrophobic compounds, fluorene and naphthalene, in all matrices (Table 1). In the silica column, the elution order of the three PAHs in the presence of 500 mg/l rhamnolipid was even reversed compared to the elution order when no rhamnolipid was present (Table 1, Fig. 2). At a concentration of 500 mg/l, rhamnolipid did not reduce

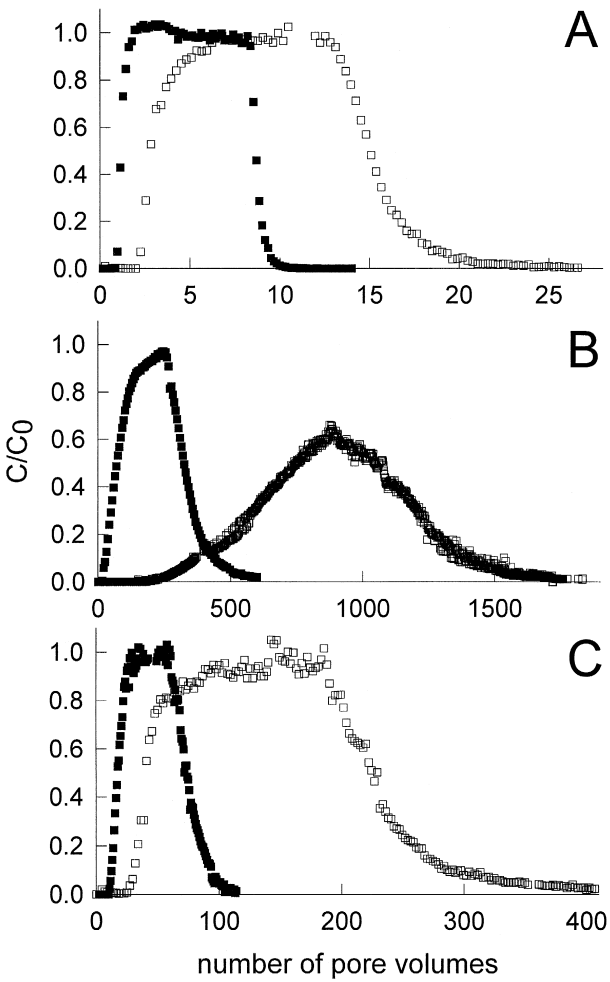

Fig. 3. Facilitated transport of phenanthrene by rhamnolipid. Breakthrough curves of phenanthrene (□), and of phenanthrene in the presence of 500 mg/l rhamnolipid (■) for silica (A), ODS (B), and HAS (C). C_0 is the influent concentration of phenanthrene (g/l).

the retardation factor for naphthalene in ODS, and even increased the retardation factor for this compound in HAS (Table 1). The facilitation of PAH transport by rhamnolipid was subsequently investigated by an analysis of the separate processes that determine the (facilitated) transport of PAH and a quantitative prediction of the retardation factors.

3.3. Processes that determine the transport of PAH

3.3.1. Transport of PAH was independent of the presence of other PAHs

In order to quantitatively describe the breakthrough curves of the individual PAHs, either in the absence or in the presence of rhamnolipid, it is important to determine whether transport of the PAHs was dependent on the presence of the other PAHs. Two observations indicate that transport of the PAHs was independent of other PAHs. First, the retardation factors, which were observed when naphthalene was present as a single component ($R = 1.65$ and 1.74 in silica, duplicate experiments) were virtually the same to the retardation factor found for naphthalene present in the PAH mixture (Table 1). Second, no overshoots in the form of a transient increase in effluent concentration to concentrations above the influent concentration were observed in the breakthrough curves of any of the components, either in the absence or in the presence of rhamnolipid (e.g., Figs. 1 and 2). Overshoots occur due to interactions between different solutes during multicomponent transport (Helfferich and Whitley, 1996). The observation that sorption of PAH was independent on the presence of other PAHs is in agreement with the apparent linearity of the isotherms (McGinley et al., 1993), but is remarkable since the adsorbed concentrations of PAHs in several experiments were high, with values up to 0.36 mg phenanthrene/mg octadecyl coating in the ODS column for the experiment without rhamnolipid. Other studies have indicated that both solubilization (Guha et al., 1998) and sorption to soil (Chiou and Kile, 1998) of hydrophobic compounds can be dependent on the presence of other hydrophobic compounds. Since sorption of the components was independent in the experiments reported here, breakthrough curves of individual compounds in the PAH mixture could be analyzed independently, i.e., without the need to account for their mutual interactions.

3.3.2. Sorption rates for PAH

The symmetric and sigmoidal breakthrough curves of the PAHs indicate that the sorption of the PAHs to these matrices was not rate-limited. Rate-limited sorption can be quantified using Damkohler numbers, which represent the ratio between the hydrodynamic residence time and the characteristic time for sorption. The Damkohler numbers that were obtained by fitting the breakthrough curves using CXTFIT (Fig. 1) were high, with values of 6 for phenanthrene in silica (one rate-limited domain), 20 for phenanthrene in ODS (one rate-limited domain), and 1.7 for phenanthrene in HAS (one instantaneous and one rate-limited domain, fraction of sorbent for which sorption was rate limited = 0.37). The Damkohler numbers show that the desorption rates were too high to be accurately quantified. However, the rate constants ($0.1–10\ h^{-1}$) are of a similar magnitude as rate constants for hydrophobic organic compounds that have been reported in earlier work with similar matrices (Szecsody and Bales, 1989; Huang and Weber, 1997b). Since transport of the PAH components was independent and not

rate-limited, the most relevant parameter to characterize PAH transport in our experiments was the retardation factor for the PAHs. These retardation factors were expected to be influenced by rhamnolipid through solubilization and admicellar sorption.

3.3.3. Solubilization of PAH by rhamnolipid

The solubilization of PAH by rhamnolipid was determined in independent experiments by measuring the increase in apparent solubility of the PAHs in rhamnolipid solutions. Rhamnolipid enhanced the apparent solubility of all PAHs in the order of naphthalene < fluorene < phenanthrene (Fig. 4). The CMC of the rhamnolipid mixture was found to be 23 ± 6 mg/l. No enhanced solubility of PAH was detected at rhamnolipid concentrations below the CMC (Fig. 4). The micelle–water partitioning constants for phenanthrene were equivalent to previously reported values (Zhang et al., 1997; Noordman et al., 1998). The observed values were similar to partitioning constants reported for synthetic surfactants (Edwards et al., 1991; Tiehm, 1994).

3.3.4. Adsorption of rhamnolipid

Since the facilitated transport of contaminants is influenced by adsorption of the facilitating agent, it is necessary to determine the adsorption of this agent for predicting its effect on contaminant transport. The amount of rhamnolipid adsorbed to the matrices was determined from the breakthrough curves of the individual rhamnolipid components (Table 1). Frontal limbs of the breakthrough curves were measured during saturation of columns with rhamnolipid and distal limbs were measured after the transport of PAH in the presence of rhamnolipid had been determined. The retardation factors for the rhamnolipid components were lower at an influent concentration of 500 mg/l rhamnolipid than at 20 mg/l rhamnolipid in all matrices, indicative of concave isotherms (Table 3). Since the retardation factors for the rhamnolipid components at an influent concentration of 500 mg/l were less than 1 in the silica column, and since retardation factors in this column were higher in the presence of 20 mM KCl (data not shown), it can be

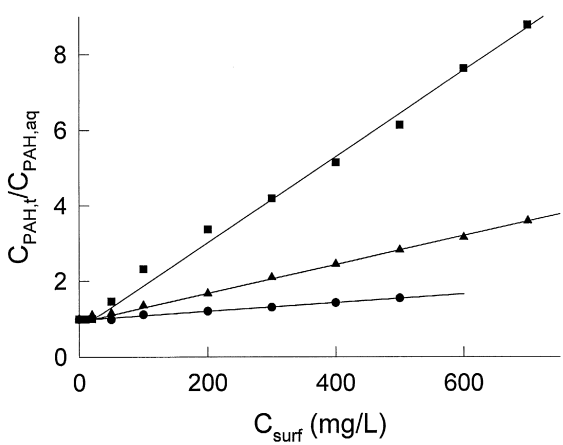

Fig. 4. Apparent solubility of naphthalene (●), fluorene (▲), and phenanthrene (■) in rhamnolipid-containing solutions. The solid line indicates the fit of the data to Eq. (1).

Table 3
Retardation factors for the two most abundant rhamnolipid components

Matrix	Rhamnolipid concentration (mg/l)	Retardation factor	
		C20RL2[a]	C20RL1[b]
Silica	20	1.8	21.8
	500	0.9	0.9
ODS	20	44	43
	500	3.5	7.6
HAS	20	33	33
	500	12	21

[a] 2-*O*-α-L-rhamnopyranosyl-α-L-rhamnopyranosyl-β-hydroxydecanoyl-β-hydroxydecanoate.
[b] α-L-rhamnopyranosyl-β-hydroxydecanoyl-β-hydroxydecanoate (Noordman et al., 2000).

concluded that rhamnolipid micelles were partly excluded from the silica pores by anion exclusion, just as described above for pentafluorobenzoic acid. It is not expected that the low observed retardation factors for rhamnolipid were caused by size exclusion, based on adsorption data for Triton X100 on silica (Giordano et al., 1993).

The retardation factors for the rhamnolipid components in ODS and HAS columns were much higher than in silica, indicating that the adsorption of rhamnolipid to these matrices was mainly caused by the octadecyl and humic acid coatings, respectively. The retardation factors for the rhamnolipid components with the HAS column were higher than with the ODS column, in contrast to what was found for the PAHs. This indicated that the hydrophobicity of the matrix was less important for adsorption of rhamnolipid than for sorption of PAH. The retardation of the individual rhamnolipid components increased with increasing hydrophobicity (Table 3). This was also observed for sandy soils and was attributed to the formation of surface aggregates by rhamnolipid (Noordman et al., 2000). Because the contribution of the individual components to solubilization and admicellar sorption of PAH was unknown, the aqueous and adsorbed concentrations of total rhamnolipid (Table 1) rather than the concentrations of the individual components were used to quantify solubilization and admicellar sorption in the rest of this study.

3.3.5. Admicellar sorption

Sorption and transport of PAH can be affected by surfactants due to admicellar sorption, which is the partitioning of components between an aqueous phase and an adsorbed surfactant phase (Valsaraj, 1989; Park and Jaffé, 1993; Monticone et al., 1994; Sun et al., 1995; Noordman et al., 1998). The occurrence of admicellar sorption in the column experiments was apparent from the retardation factors reported in Table 1 for the following reasons: (1) the retardation factors for phenanthrene in silica were higher with a mobile phase containing 20 and 50 mg/l rhamnolipid than with a mobile phase containing no rhamnolipid; (2) the retardation factor of naphthalene in ODS was higher in the presence of 20 mg/l rhamnolipid than when rhamnolipid was absent; (3) the retardation factors for naphthalene in HAS were significantly higher in the presence of rhamnolipid; and (4) the retardation factor for phenanthrene in HAS was larger than

predicted from solubilization when admicellar sorption was not taken into account. In the latter case, the retardation factor would have been reduced by a factor of $1 + K_c C_{mic}$ (Noordman et al., 1998), which is equal to 6.7 at 500 mg/l rhamnolipid. The rhamnolipid surfactant thus influenced sorption of hydrophobic components both by solubilization and by admicellar sorption. These opposing effects of surfactants on the transport of solutes are also known from liquid chromatography, where the presence of surfactants in the mobile phase can increase the retardation of certain solutes when used at submicellar concentrations but decrease retardation when used at supramicellar concentrations (Kord and Khaledi, 1992).

3.4. Quantitative analysis of retardation factors

3.4.1. Estimation of retardation factors

The retardation factors for the PAHs in the presence of rhamnolipid at supramicellar concentrations were estimated from the previously determined parameters (Tables 1 and 2) and surfactant concentrations (Table 1) using Eq. (3) (Johnson et al., 1998; Noordman et al., 1998).

$$R = 1 + \frac{\rho}{\theta} \frac{K_d + K_{ad} S_{surf}}{1 + K_c C_{mic}}, \tag{3}$$

K_{ad} (l/g) is the admicellar partitioning constant (Valsaraj and Thibodeaux, 1989; Noordman et al., 1998). This constant is defined by the relation $K_{ad} = S_{PAH,ad} C_{PAH,aq}^{-1} S_{surf}^{-1}$, where $S_{PAH,ad}$ is the concentration of PAH bound to sorbed surfactant (g PAH/kg matrix). It was assumed that $K_{ad} = K_c$ (vide infra). Since the composition of rhamnolipid in the aqueous phase during the column experiments with PAH was equal to the composition of the original mixture, the micelle-partitioning constants that were determined with the original mixture could also be used for the description of column experiments. When $C_{mic} = S_{surf} = 0$, Eq. (3) reduces to Eq. (2).

The retardation factors for PAH in silica were observed and predicted to first increase with increasing rhamnolipid concentration and to subsequently decrease at concentrations well above the CMC (Table 1, Fig. 2). The predicted retardation factors in the presence of 500 mg/l rhamnolipid matched the experimental values for PAH in silica and ODS and for phenanthrene in HAS. Thus, the facilitated transport of PAH by rhamnolipid could be reasonably well predicted by accounting for sorption, admicellar sorption, and solubilization by using independently obtained K_c and K_d values. This suggests that Eq. (3) provides an accurate description of the facilitated transport process. However, two systematic deviations between the observed and predicted retardation factors for PAH in the presence of rhamnolipid merit further attention.

3.4.2. High admicellar sorption for PAHs with low hydrophobicity

A first deviation between the observed and predicted retardation factors was seen for naphthalene and fluorene with the HAS column in the presence of 500 mg/l rhamnolipid and for naphthalene with the ODS column in the presence of 20 and 500 mg/l rhamnolipid. In these cases, the observed retardation factors were larger than predicted with Eq. (3) (Table 1). This may indicate that the amount of admicellar-sorbed solute

was higher than predicted assuming $K_{ad} = K_c$ for the less hydrophobic compounds naphthalene and fluorene. The LFERs between log K_c and log K_{ow}, that is discussed in Section 3.4.4, and between log K_{ad} and log K_{ow}, derived in Section 3.5, indeed indicate that the effect of admicellar sorption on retardation factors is expected to be more pronounced for the less hydrophobic compounds (vide infra).

3.4.3. Adsorbed rhamnolipid reduces the affinity of fluorene and phenanthrene for ODS

A second deviation between the observed and predicted retardation factors was noticed for fluorene and phenanthrene in the presence of rhamnolipid in ODS. The observed retardation factors were considerably smaller than predicted (Table 1). In the presence of 20 mg/l rhamnolipid, the retardation factors for fluorene and phenanthrene in ODS were a factor 2.2 and 2.8 lower compared to the retardation factors determined in the absence of rhamnolipid (Table 1). This reduction in retardation factors cannot be explained by solubilization of PAH by rhamnolipid, since no solubilization was observed at 20 mg/l rhamnolipid (Fig. 3). Therefore, the reduced sorption of PAH to ODS in the presence of rhamnolipid must be caused by a negative effect of adsorbed surfactant on the ODS–water partitioning constants of PAH. This effect outweighed the effect of admicellar sorption for fluorene and phenanthrene but not for naphthalene.

The reduction by surfactants of the ODS–water partitioning constants of organic compounds has also been observed in micellar liquid chromatography (Khaledi and Breyer, 1989; Lavine et al., 1994). The effect of rhamnolipid can be quantitatively compared to the effect of sodium dodecylsulfate (SDS) since the retardation factors for PAHs with a SDS-modified stationary ODS have been estimated from retardation factors determined at SDS concentrations above the CMC by extrapolation to zero micelle concentration (Arunyanart and Cline Love, 1984; Borgerding et al., 1988; González et al., 1992). The estimated retardation factors for fluorene and phenanthrene in SDS-modified ODS at zero micelle concentration were 175 and 259, respectively (recalculated from data presented by González et al. (1992) for a column with 1.6% ODS, w/w). For anthracene, a compound with a K_{ow} almost equal to that of phenanthrene (Schwarzenbach et al., 1993), the estimated retardation factor in SDS-modified ODS was 180 (recalculated for a column with 1.6% ODS, w/w, from data presented by Arunyanart and Cline Love (1984)). These values are close to the observed retardation factors of fluorene and phenanthrene in the presence of 20 mg/l rhamnolipid (Table 1), indicating that adsorbed rhamnolipid and adsorbed SDS show a similar reduction of the affinity of PAH to surfactant-modified ODS.

The retardation factors for fluorene and phenanthrene in the ODS columns were probably reduced by rhamnolipid due to a negative effect of the polar rhamnose units and the anionic carboxylate moiety of rhamnolipid on the hydrophobicity the coating. The same was proposed to occur in micellar liquid chromatography (González et al., 1992; Lavine et al., 1994). The reduced affinity for ODS in the presence of adsorbed surfactants can be explained by the observation that the hydrophobicity of aliphatic moieties is reduced by ionic groups in their vicinity (Noordman et al., 1993; Hol et al., 1997). The fact that this transport-facilitating effect of surfactants at submicellar concentrations was not observed with silica or HAS suggests that it will only be important for very hydrophobic matrices such as ODS.

3.4.4. Linear free-energy relations

LFERs were used to determine the dependence of the partitioning constants on the hydrophobicity of the contaminants, as described by the logarithm of the 1-octanol–water partitioning coefficient K_{ow} (Schwarzenbach et al., 1993). The logarithm of the matrix–water partitioning constants correlated well with the log K_{ow} values ($r^2 > 0.992$, Table 2, Fig. 5). The slope of the log K_d–log K_{ow} plots increased in the order of silica < HAS < ODS, showing that the partitioning constants for PAH increased more strongly with contaminant hydrophobicity for ODS than for HAS and silica. The low slope for silica (0.4) was similar to the slope observed for glass (Lion et al., 1990), and reflects the fact that both these materials are hydrophilic. The slope for ODS was higher than 1, which indicated that the surface was more hydrophobic than 1-octanol. The slope for HAS was similar to values commonly observed for soils and sediments (Sabljic, 1987) and similar to the slope of 1.07 ($n = 10$, $r^2 = 0.96$) that we calculated for HAS prepared by Szabó and Bulman (1994). The retention data that were used to calculate the latter slope were reported by Szabó and Bulman (1994) and the K_{ow} values were taken from Schwarzenbach et al. (1993). The higher slope for ODS than for HAS reflects the higher K_{oc} values observed with ODS than with HAS (Table 2).

The micelle–water partitioning constants for the PAHs were also correlated with the 1-octanol–water partitioning constants of the solutes (Table 2, Fig. 5). The slope of the log K_c–log K_{ow} plot was lower than 1, indicating a lower effect of solute hydrophobicity on micellar partitioning than on 1-octanol–water partitioning. The slope was similar to slopes of log K_c–log K_{ow} plots obtained with SDS, sodium dodecylbenzenesulfonate, and hexadecyltrimethylammonium bromide micelles (Valsaraj and Thibodeaux, 1989) and with Triton $\times 100$ micelles (Edwards et al., 1991). This indicates that the dependence of K_c on K_{ow} is the same for a wide range of surfactants, including rhamnolipid.

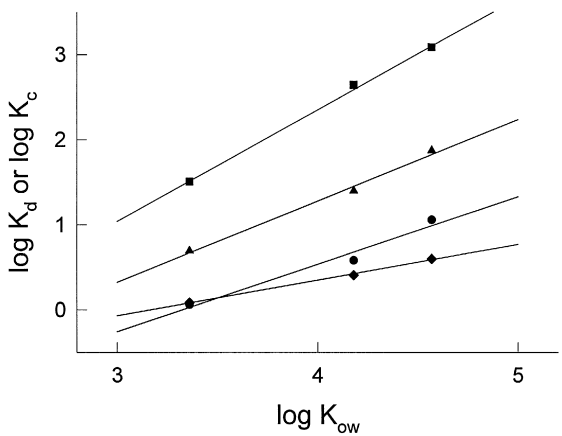

Fig. 5. Dependence of the matrix–water partitioning constants (K_d, l/kg) and micelle–water partitioning constants (K_c, l/g) for naphthalene, fluorene, and phenanthrene on their 1-octanol–water partitioning constants. Values for log K_d for silica (♦), ODS (■), and HAS (▲), and log K_c (●) as a function of log K_{ow}. Solid lines were obtained by linear regression.

3.5. General prediction of transport facilitation of hydrophobic compounds by surfactants

The LFERs presented in the previous paragraph indicate that the partitioning constants of PAHs were strongly correlated to their K_{ow} values. Therefore, Eq. (3) can be rewritten by substitution of K_c, K_{ad}, and K_c for the corresponding LFERs:

$$R = 1 + \frac{\rho}{\theta} \frac{AK_{ow}^{a} + BK_{ow}^{b} S_{surf}}{1 + CK_{ow}^{c} C_{mic}} \tag{4}$$

where A, B, and C are the intercepts and a, b, and c are slopes of the plots of log K_d, log K_{ad}, and log K_c with log K_{ow}, respectively. Eq. (4) gives the retardation factor for a compounds as a function of its K_{ow} value and the surfactant concentration. This equation will now be used to make a general prediction of the facilitated transport of hydrophobic organic compounds by surfactants. The values used for this simulation were obtained from the LFERs in this study. Values for A and a were obtained from the intercepts and slopes, respectively, of the log K_d–log K_{ow} plot with K_d values from the HAS column (Table 2). Values for C and c were obtained from the intercepts and slopes, respectively, of the log K_c–log K_{ow} plot with K_c values derived from the solubilization data of PAH by rhamnolipid (Table 2). Values for S_{surf} were calculated at each surfactant concentration using a Langmuir isotherm using $S_{max} = 1.0$ g/kg and $K_L = 100$ l/g, which are realistic values for rhamnolipid adsorption to soil (Noordman et al., 1998).

To obtain values for B and b, the intercepts and slopes were calculated of a log K_{ad}–log K_{ow} plot of a set of literature data describing the admicellar sorption of organic compounds with log K_{ow} values between 0.9 and 6.7, with cationic, anionic, and nonionic surfactants both at supra and submicellar concentrations that were adsorbed to different types of matrices (Fig. 6, Eq. (5)).

$$\log K_{ad} = 0.708 \log K_{ow} - 2.03 \quad n = 31, r^2 = 0.82. \tag{5}$$

The admicellar partitioning constant K_{ad} depends on the compound hydrophobicity (Lee et al., 1990; Park and Jaffé, 1993; Nayyar et al., 1994; Sun et al., 1995), surfactant type (Esumi et al., 1997), concentration of surfactant (Lee et al., 1990; Edwards et al., 1994), and type of matrix (Esumi et al., 1997). Despite these numerous dependencies, the data show that log K_{ad} generally increases as a linear function of log K_{ow}. The slope of the log K_{ad}–log K_{ow} plot was smaller than the slopes of log K_c–log K_{ow} plots (Table 2; Valsaraj and Thibodeaux, 1989; Edwards et al., 1991). The smaller slope indicates that admicellar partitioning increases with contaminant hydrophobicity to a smaller extent than micellar solubilization, which has been reported previously for several specific cases (Park and Jaffé, 1993; Nayyar et al., 1994; Zhu et al., 1998). This might be caused by the greater rigidity or smaller aggregate size of admicelles compared to micelles (Park and Jaffé, 1993) or to the affinity of the less hydrophobic compounds to the perimeter of incompletely formed admicelles where the hydrophobic surfactant tails are exposed to the aqueous phase (Lee et al., 1990; Nayyar et al., 1994).

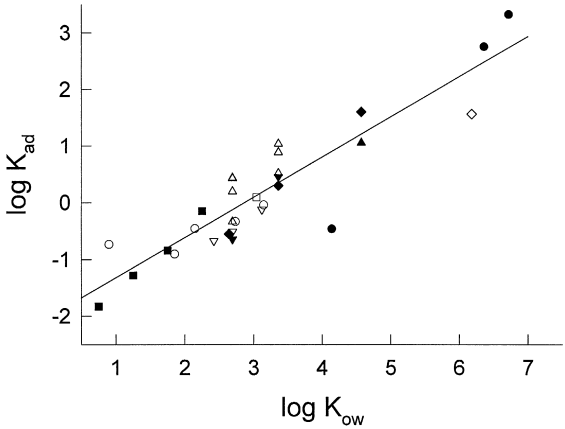

Fig. 6. The admicellar partitioning constant (K_{ad}, l/g) as a function of solute K_{ow}. The solid line was obtained by linear regression. Data were taken from Sun et al. (1995) (●), Lai et al. (1997) (■), Edwards et al. (1994) (▲), Nayyar et al. (1994) (▼), Park and Jaffé (1993) (◆), Zhu et al. (1998) (○), Kitiyanan et al. (1996) (□), Esumi et al. (1997) (△), Holsen et al. (1991) (▽), Hunter et al. (1996) (◇).

The retardation factors that were predicted by Eq. (4) increased with increasing surfactant concentration up to the CMC of 20 mg/l due to admicellar sorption, for all values of K_{ow} (Fig. 7). With a further increase in surfactant concentration, retardation factors decreased due to solubilization. The decrease in retardation factors in the presence of 500 mg/l surfactant compared to the retardation factors in the absence of

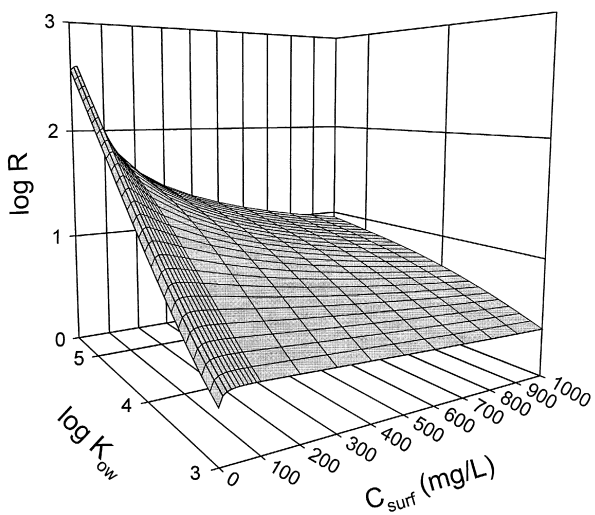

Fig. 7. Simulation of facilitated transport. The graph shows retardation factors for contaminants as a function of contaminant K_{ow} and surfactant concentration C_{surf}. Retardation factors were predicted with Eq. (4) as explained in the text. Mesh lines are drawn every 20 mg/l in the range of C_{surf} between 0 and 100 mg/l, every 100 mg/l in the range of C_{surf} between 100 and 900 mg/l, and at each interval of 0.1 log K_{ow} unit.

surfactant was more that 10-fold for contaminants with log $K_{ow} > 5$. However, the retardation factors for less hydrophobic compounds (log $K_{ow} < 3.5$) in the presence of 500 mg/l surfactant was higher that the retardation factor in the absence of surfactant, showing that for these compounds the negative effects of admicellar sorption were not overcome by the positive effects of solubilization by 500 mg/l surfactant.

Retardation factors increased to a lesser degree with an increase in K_{ow} at high surfactant concentrations than when no surfactant was present (Fig. 7). This can be explained by realizing that, when solubilization plays an important role (i.e., $CK_{ow}^{c} C_{mic} \gg 1$), Eq. (5) reduces to:

$$R \approx XK_{ow}^{(x-c)} \tag{6}$$

where X is a constant and $x = a$ when $AK_{ow}^{a} \gg BK_{ow}^{b} S_{surf}$, and $x = b$ when $AK_{ow}^{a} \ll BK_{ow}^{b} S_{surf}$. Eq. (6) implies that when x and c are similar, as was the case for the simulation shown in Fig. 7, retardation factors become increasingly less dependent on K_{ow} at higher surfactant concentrations. This was also predicted for facilitated transport by SDS (Valsaraj and Thibodeaux, 1989) and by dissolved organic matter (Kan and Tomson, 1990), and has been observed in micellar liquid chromatography (Khaledi and Breyer, 1989). Therefore, the decreased dependence of the retardation factor of compounds on their K_{ow} in the presence of solubilizing agents seems to be a general fact. This fact implies that these solubilizing agents are especially effective for facilitating the transport of hydrophobic contaminants. When $c > x$ and when the surfactant concentration is high, the retardation factors for a series of compounds can be inversely related to their K_{ow}, as was observed for the PAHs in silica in the presence of 500 mg/l rhamnolipid ($c = 0.8$, $x = 0.4$). The competing effects of solubilization, admicellar sorption, and sorption of the contaminant determine the suitability of surfactants to facilitate transport of soil contaminants.

4. Conclusions

The retardation factors for PAH in all matrices and their reduction by rhamnolipid were mainly dependent on the hydrophobicity of the contaminants. The 1-octanol–water partitioning constants for contaminants could be used to describe their sorption, solubilization, and admicellar sorption. These latter processes determine the degree to which (bio)surfactants can enhance the removal of soil contaminants under equilibrium conditions. The use of surfactants is most promising for enhancing the removal of the more hydrophobic compounds whereas the effectiveness of surfactants for enhancing removal of the less hydrophobic compounds may considerably be reduced by admicellar sorption. Of course, the effectiveness of surfactants for contaminant removal from soils may also be limited by the existence of non-equilibrium conditions (Noordman yet al., 1998).

Acknowledgements

This research was funded by the Dutch IOP Environmental Biotechnology Program (contract number IOP91224). R. Eendhuizen is acknowledged for determining the

micelle–water partitioning constants. Dr. J.T. Trevors is acknowledged for making strain UG2 available for our research.

References

Arunyanart, M., Cline Love, L.J., 1984. Model for the micellar effects on liquid chromatography capacity factors and for determination of micelle-solute equilibrium constants. Anal. Chem. 56, 1557–1561.

Bai, G.-Y., Brusseau, M.L., Miller, R.M., 1997. Biosurfactant-enhanced removal of residual hydrocarbon from soil. J. Contam. Hydrol. 25, 157–170.

Borgerding, M.F., Quina, F.H., Hinze, W.L., Bowermaster, J., McNair, H.M., 1988. Investigation of the retention mechanism in nonionic micellar liquid chromatography using an alkylbenzene homologous series. Anal. Chem. 60, 2520–2527.

Burris, D.R., Antworth, C.P., Stauffer, T.B., MacIntyre, W.G., 1991. Humic acid-modified silica as a model aquifer material. Environ. Toxicol. Chem. 10, 433–444.

Buszewski, B., Gadzala-Kopciuch, R.M., Markuszewski, M., Kaliszan, R., 1997. Chemically bonded silica stationary phases: synthesis, physicochemical characterization, and molecular mechanism of reversed phase HPLC retention. Anal. Chem. 69, 3277–3284.

Chin, Y.P., Peven, C.S., Weber, W.J. Jr., 1988. Estimating soil/sediment partition coefficients for organic compounds by high performance reverse phase liquid chromatography. Water Res. 22, 873–881.

Chiou, C.T., Kile, D.E., 1998. Deviations from sorption linearity on soils of polar and nonpolar organic compounds at low relative concentrations. Environ. Sci. Technol. 32, 338–343.

Das, B.S., Kluitenberg, G.J., 1996. Moment analysis to estimate degradation rate constants from leaching experiments. Soil Sci. Soc. Am. J. 60, 1724–1731.

Edwards, D.A., Luthy, R.G., Liu, Z., 1991. Solubilization of polycyclic aromatic hydrocarbons in micellar nonionic surfactant solutions. Environ. Sci. Technol. 25, 127–133.

Edwards, D.A., Adeel, Z., Luthy, R.G., 1994. Distribution of nonionic surfactant and phenanthrene in a sediment/aqueous system. Environ. Sci. Technol. 28, 1550–1560.

Esumi, K., Uda, S., Suhara, T., Fukui, H., Koide, Y., 1997. Cationic surfactant adsolubilization of 2-naphthol and naphthalene with titanium dioxide having dodecyl chain. J. Colloid Interface Sci. 193, 315–318.

Fortin, J., Jury, W.A., Anderson, M.A., 1997. Enhanced removal of trapped nonaqueous phase liquids from saturated soil using surfactant solutions. J. Contam. Hydrol. 24, 247–267.

Giordano, F., Denoyel, R., Rouquerol, J., 1993. Influence of porosity on the adsorption of a nonionic surfactant on silica. Colloids Surf. A 71, 293–298.

González, V., Rodríguez-Delgado, M.A., Sánchez, M.J., Garciá-Montelongo, F., 1992. Solute-micelle association constants and correlation of octanol–water coefficients with hydrophobicity for polycyclic aromatic hydrocarbons by micellar chromatography. Chromatographia 34, 627–635.

Guha, S., Jaffé, P.R., Peters, C.A., 1998. Solubilization of PAH mixtures by a nonionic surfactant. Environ. Sci. Technol. 32, 930–935.

Helfferich, F.G., Whitley, R.D., 1996. Nonlinear-waves in chromatography: 2. Wave interference and coherence in multicomponent systems. J. Chromatogr., A 734, 7–47.

Hol, P., Streefland, L., Blandamer, M.J., Engberts, J.B.F.N., 1997. Kinetic medium effects of cationic cosolutes in aqueous solution: the effects of alkylammonium bromides on the neutral hydrolysis of 1-benzoyl-1,2,4-triazole. J. Chem. Soc., Perkin Trans. 2, 485–488.

Holsen, T.M., Taylor, E.R., Seo, Y.C., Anderson, P.R., 1991. Removal of sparingly soluble organic chemicals from aqueous solutions with surfactant-coated ferrihydrite. Environ. Sci. Technol. 25, 1585–1589.

Huang, W.L., Weber, W.J., 1997a. A distributed reactivity model for sorption by soils and sediments: 10. Relationships between desorption, hysteresis, and the chemical characteristics of organic domains. Environ. Sci. Technol. 31, 2562–2569.

Huang, W.L., Weber, W.J., 1997b. Thermodynamic considerations in the sorption of organic contaminants by soils and sediments: 1. The isosteric heat approach and its application to model inorganic sorbents. Environ. Sci. Technol. 31, 3238–3243.

Hunter, M.A., Kan, A.T., Tomson, M.B., 1996. Development of a surrogate sediment to study the mechanisms responsible for adsorption/desorption hysteresis. Environ. Sci. Technol. 30, 2278–2285.

Johnson, W.P., Cabral, K., Lion, L.W., Corapcioglu, Y.M., 1998. Reconciliation of expressions for the modified retardation factor and incorporation of non-linear contaminant sorption to the stationary phase. J. Contam. Hydrol. 32, 247–266.

Kan, A.T., Tomson, M.B., 1990. Ground water transport of hydrophobic organic compounds in the presence of dissolved organic matter. Environ. Toxicol. Chem. 9, 253–263.

Khaledi, M.G., Breyer, E.D., 1989. Quantitation of hydrophobicity with micellar liquid chromatography. Anal. Chem. 61, 1040–1047.

Kitiyanan, B., O'Haver, J.H., Harwell, J.H., Osuwan, S., 1996. Absolubilization of styrene and isoprene in cetyltrimethylammonium bromide admicelle on precipitated silica. Langmuir 12, 2162–2168.

Klavins, M., 1993. Immobilization of humic substances. Latv. Kim. Z. 1, 96–102.

Kord, A.S., Khaledi, M.G., 1992. Chromatographic characteristics of surfactant-mediated separations: micellar liquid chromatography vs. ion pair chromatography. Anal. Chem. 64, 1901–1907.

Lai, C.L., O'Rear, E.A., Harwell, J.H., Hwa, M.J., 1997. Adsolubilization of fluorocarbon alcohols into perfluoroheptanoate admicelles formed on alumina. Langmuir 13, 4267–4272.

Lavine, B.K., Hendayana, S., Teteault, J., 1994. Selectivity in micellar reversed-phase liquid chromatography: C−18 and C−8 alkyl bonded phases. Anal. Chem. 66, 3458–3465.

Lee, C., Yeskie, M.A., Harwell, J.H., O'Rear, E.A., 1990. Two-site adsolubilization model of incorporation of alcohols into adsorbed surfactant aggregates. Langmuir 6, 1758–1762.

Lion, L.W., Stauffer, T.B., MacIntyre, W.G., 1990. Sorption of hydrophobic compounds on aquifer materials: analysis methods and the effect of organic carbon. J. Contam. Hydrol. 5, 215–234.

McGinley, P.M., Katz, L.E., Weber, W.J., 1993. A distributed reactivity model for sorption by soils and sediments: 2. Multicomponent systems and competitive effects. Environ. Sci. Technol. 27, 1524–1531.

Monticone, V., Mannebach, M.H., Treiner, C., 1994. Coadsorption of 2-naphtol and cetylpyridinium chloride at a silica/water interface in relation with the micellar solubilization effect. Langmuir 10, 2395–2398.

Mulder, H., Wassink, G.R., Breure, A.M., Van Andel, J.G., Rulkens, W.H., 1998. Effect of nonionic surfactants on naphthalene dissolution and biodegradation. Biotechnol. Bioeng. 60, 397–407.

Nayyar, S.P., Sabatini, D.A., Harwell, J.H., 1994. Surfactant adsolubilization and modified admicellar sorption of nonpolar, polar and ionizable organic contaminants. Environ. Sci. Technol. 28, 1874–1881.

Nielsen, T., Siigur, K., Helweg, C., Jorgensen, O., Hansen, P.E., Kirso, U., 1997. Sorption of polycyclic aromatic-compounds to humic-acid as studied by high-performance liquid chromatography. Environ. Sci. Technol. 31, 1102–1108.

Noordman, W.H., Blokzijl, W., Engberts, J.B.F., Blandamer, M.J., 1993. Kinetic medium effects of amphiphilic cosolutes below their critical micelle concentration: the effect of sodium *n*-alkyl sulfates on the neutral hydrolysis of 1-benzoyl-1,2,4-triazole. J. Org. Chem. 58, 7111–7114.

Noordman, W.H., Ji, W., Brusseau, M.L., Janssen, D.B., 1998. Effects of rhamnolipid biosurfactants on removal of phenanthrene from soil. Environ. Sci. Technol. 32, 1806–1812.

Noordman, W.H., Brusseau, M.L., Janssen, D.B., 2000. Adsorption of a multicomponent rhamnolipid surfactant to soil. Environ. Sci. Technol. 34, 832–838.

Park, J.-W., Jaffé, P.R., 1993. Partitioning of three nonionic organic compounds between adsorbed surfactants, micelles, and water. Environ. Sci. Technol. 27, 2559–2656.

Parker, J.C., Van Genuchten, M.T., 1984. Determining transport parameters from laboratory and field tracer experiments. Bulletin 84-3, Virginia Agricultural Experiment Station (Blacksburg).

Sabljic, A., 1987. On the prediction of soil sorption coefficients of organic pollutants from molecular structure: application of molecular topology model. Environ. Sci. Technol. 21, 358–366.

Sahoo, D., Smith, J.A., 1997. Enhanced trichloroethene desorption from long-term contaminated soil using Triton X-100 and pH increases. Environ. Sci. Technol. 31, 1910–1915.

Schwarzenbach, R.P., Gschwend, P.M., Imboden, D.M., 1993. Environmental Organic Chemistry. 1st edn. Wiley, New York, 681 pp.

Sun, S., Inskeep, W.P., Boyd, S.A., 1995. Sorption of nonionic organic compounds in soil–water systems containing a micelle-forming surfactant. Environ. Sci. Technol. 29, 903–913.

Szabó, G., Bulman, R.A., 1994. Comparison of adsorption coefficient (KOC) for soils and HPLC retention

factors of aromatic hydrocarbons using a chemically immobilized humic acid column in RP-HPLC. J. Liq. Chromatogr. 17, 2593–2604.

Szabó, G., Angelova, A., Guczi, J., Bulman, R.A., 1993. An examination of the uptake of radioiodide by chemically bound humic acid and by some solid phases of soil. Sci. Total Environ. 130–131, 375–382.

Szecsody, J.E., Bales, R.C., 1989. Sorption of low-molecular-weight hydrophobic organic compounds on surface-modified silica. J. Contam. Hydrol. 4, 181–203.

Tiehm, A., 1994. Degradation of polycyclic aromatic hydrocarbons in the presence of synthetic surfactants. Appl. Environ. Microbiol. 60, 258–263.

Valsaraj, K.T., 1989. Partitioning of hydrophobic nonpolar volatile organics between the aqueous and surfactant aggregate phases on alumina. Sep. Sci. Technol. 24, 1191–1205.

Valsaraj, K.T., Thibodeaux, L.J., 1989. Relationships between micelle–water and octanol–water partition constants for hydrophobic organics of environmental interest. Water Res. 23, 183–189.

Zhang, Y., Maier, W.J., Miller, R.M., 1997. Effect of rhamnolipids on the dissolution, bioavailability, and biodegradation of phenanthrene. Environ. Sci. Technol. 31, 2211–2217.

Zhu, L.Z., Ren, X.G., Yu, S.B., 1998. Use of cetyltrimethylammonium bromide-bentonite to remove organic contaminants of varying polar character from water. Environ. Sci. Technol. 32, 3374–3378.